LHCb Note 2003-048
TRIG

LEVEL-0 TRIGGER
BANDWIDTH DIVISION

E. Rodrigues

eduardo.rodrigues@cern.ch

CERN

September 2003

Abstract

The Level-0 trigger bandwidth division is described in detail: motivations from the physics performance point of view, technical implementation, and results obtained for the Trigger System Technical Design Report.

1 Introduction

The significance of a measurement performed on a given B-meson decay channel will directly depend on the corresponding reconstruction efficiency and therefore on the Level-0 (L0) trigger efficiency, $\varepsilon_{\mathrm{L0}}^{channel}$, the fraction of offline selected events [1] that pass L0.

The maximization of the L0 performance for offline selected events is done by optimizing the bandwidth given to each of the sub-triggers based on: hadron, electron, photon, muon and π^0 L0 candidates. In other words, it depends on the trigger rates allocated to each of these sub-triggers – the bandwidth division.

In the next section I first remind the changes introduced recently in the L0 Decision Unit algorithm. Follows the body of the note explaining how the bandwidth division studies were done – basic ideas and implementation. Section 4 describes the data samples used and the simulation framework. The final section presents and discusses all the results.

2 L0 Decision Unit Algorithm

In the past few months several changes were made to the L0 Decision Unit (L0DU): new cuts were introduced which required an update on the algorithm.

First, it was realized the usefulness of a cut on the Scintillator Pad Detector (SPD) multiplicity in rejecting as early as possible busy events, thereby improving the physics (reconstruction) performance. Also these same events take longer to be processed by the Level-1 (L1) trigger and the High Level Trigger (HLT). This new cut on the SPD hit multiplicity was introduced in the L0 trigger both at hardware level and in the L0DU [2].

Recently a new and similar cut on the Pile-Up Veto hit multiplicity was investigated from the point of view of the L0 and L1 triggers. Due to a correlation of this multiplicity cut with the cut on the number of tracks from the second vertex (estimated by the veto's height of the second peak), all these three cuts were studied simultaneously [3]. The numbers collected in table 1 were finally chosen for providing an overall optimal L0×L1 efficiency for several channels. Further details can be found in [3]. These three cuts and the total E_{T} cut – $\sum E_{\mathrm{T}}$, a measure of the total energy in the hadronic calorimeter – will hereafter be referred to as the global event variables.

At present the L0DU algorithm issues a trigger decision based on the global event variables and on the transverse energies reconstructed by the hadron, electron, photon, muon, di-muon and π^0 local and global triggers. Note that the di-muon trigger sums the transverse momenta of the two highest p_{T} muons – $\Sigma p_{\mathrm{T}}^{\mu}$ – without the requirement that

---

[1] The list of channels and corresponding offline selections are in accordance with those described in the LHCb Reoptimized Detector Design and Performance Technical Design Report [1] and references therein.

both their values are greater than zero, i. e. it is equivalent to the muon trigger if only one muon was found in the event.

The L0DU algorithm was changed accordingly: an event triggers L0 if

1. and only if the $\sum E_{\mathrm{T}}$ is above 5.0 GeV, and
2. it passes the global event selection and at least one of the L0 candidates passes its E_{T} threshold, or
3. if $\Sigma p_{\mathrm{T}}^{\mu}$ (di-muon trigger) is above its threshold, irrespective of the global event cuts (only the $\sum E_{\mathrm{T}}$ cut is applied).

3 Bandwidth Division

3.1 Philosophy

As stated above, the optimization of the bandwidth division consists in finding the sharing of the rates allocated to the various sub-triggers in such a way as to maximize the L0 performance. But what exactly should our performance criteria be? Ultimately it will always be a matter of choice and convention.

LHCb is primarily designed to study in detail the CKM matrix and B-hadrons rare decays. We opted to characterize the performance of L0 with a set of channels which are representative both in giving access to the CKM parameters, and in the way they rely on the different trigger components. The following channels were selected:

$\mathrm{B_d^0} \to \pi^+\pi^-$,
$\mathrm{B_d^0} \to \mathrm{J}/\psi(\mathrm{e^+e^-}/\mu^+\mu^-)\mathrm{K_S^0}(\pi^+\pi^-)$,
$\mathrm{B_s^0} \to \mathrm{D_s^-}(\mathrm{K^+K^-}\pi^-)\mathrm{K^+}, \mathrm{D_s^-}(\mathrm{K^+K^-}\pi^-)\pi^+$,
$\mathrm{B_s^0} \to \mathrm{J}/\psi(\mu^+\mu^-)\phi(\mathrm{K^+K^-})$ and
$\mathrm{B_d^0} \to \mathrm{K^{*0}}(\mathrm{K^+}\pi^-)\gamma$.

The L0 bandwidth division proceeds in two steps. First, each channel is optimized independently, to find $\varepsilon_{\mathrm{L0-max}}^{channel}$, the maximum trigger efficiency obtainable at L0 for this channel by adjusting the thresholds to give it the whole bandwidth. Then the overall loss in efficiency is minimized. Equivalently we maximize the quantity

$$\sum_{channels} \frac{\varepsilon_{\mathrm{L0}}^{channel}}{\varepsilon_{\mathrm{L0-max}}^{channel}} \quad , \tag{1}$$

(the sum running over the above-mentioned channels), $\varepsilon_{\mathrm{L0}}^{channel}$ being the trigger efficiency using a set of thresholds for all channels simultaneously, i.e. by sharing the bandwidth between all representative channels.

In trying to obtain the best possible performance of the trigger, correlations between the different trigger levels should also be taken into account. Ideally, L0, L1 and the HLT should be optimized simultaneously. This scenario was simplified by first determining the cuts on the global event variables in a simultaneous optimization of the two first trigger levels [3], for a reasonable set of initial cuts applied at these levels.

All global event cuts were fixed to the values collected in table 1. Only the L0 E_{T} thresholds were then allowed to vary in the optimization.

The bandwidth division described above and based on the L0 efficiency is not the only possibility for a L0 optimization: as many B-decay CP-measurement and flavour oscillation studies require flavour tagging, another possibility is to optimize L0 on the trigger power rather than just considering the L0 efficiency as used above. The trigger power combines in an adequate way the trigger efficiency with the effective tagging efficiency (see, for instance, reference [4]). This alternative will be presented elsewhere [5].

3.2 Implementation

We implemented the optimizations needed to find both the $\varepsilon^{channel}_{\mathrm{L0-max}}$ of each channel and the overall loss in efficiency (cf. equation 1), in a program relying on the MINUIT minimization package [6].

The structure was defined such that the user has a total control on a certain number of important initial settings: the L0 minimum bias retention rate, the B-mesons decay channels to use, the type of optimization to do (finding of $\varepsilon^{channel}_{\mathrm{L0-max}}$ or trigger bandwidth division), optimization on the trigger efficiency or power, specification of self-tagging channels (in the case of an optimization on the trigger power), and thresholds to be fixed or varied and some other MINUIT-related settings.

We also made sure that the L0 thresholds were varied in a discrete way, in order to be as much as possible insensitive to statistical fluctuations in the trigger E_{T} distributions. This also helps in avoiding fake optimal points in the (thresholds) parameter space.

A last remark is worth pointing out: during the optimization, the whole parameter space is scanned through by MINUIT, and to each point in this space corresponds a minimum bias retention rate. A priori the latter can be arbitrary, i.e. it can differ from the retention rate corresponding to the specified initial setting – an optimization constraint.

When optimizing the performance of the L0 trigger we tried to take this constraint into account in a way as close as possible to the real data taking. In the running experiment, the trigger output is controlled and monitored. In the eventuality that the L0 output rate exceeds the nominal value, the timing and fast control will automatically overrule the L0 decision to reduce the output rate back to its nominal value. This overruling is done randomly, and will reduce on average the rate of signal events that pass L0 by the same (reduction) factor.

We applied this idea during the MINUIT optimization: for each set of thresholds returned by MINUIT the minimum bias retention is calculated and compared to the specified fixed value. If the calculated value is above, a reduction factor is computed, and then used to scale down the corresponding channel efficiencies. In case the value is lower, all variable thresholds are scaled by a common factor until the output rate is back to the required value. The efficiencies are then calculated.

4 Simulation and Data Samples

All the simulation studies were done with samples of minimum bias and B-decay signal events produced for the LHCb Trigger system and the LHCb Reoptimized Detector Design and Performance Technical Design Reports. The data were generated with Brunel v17r4, SICBMC v260r2 and database v254r1.

We obtained the bandwidth division for our nominal L0 output rate of 1.0 MHz and also repeated the exercise at 0.5, 0.7 and 0.9 MHz, to study the effect of the output rate on the trigger performance. The next paragraph presents and discusses the results.

In what follows we assumed that a L0 output rate of 1.0 MHz corresponds to a minimum bias retention of 6.74%. It was derived as follows.

The nominal L0 retention rate is defined as the ratio of the nominal output (1.0 MHz) and input rates. The L0 input rate is simply the rate of crossings with activity in the detector, i.e. with at least one interaction. We based our calculations on some LHC- and Monte Carlo-related settings:

- all LHCb simulations have been done with the PYTHIA program version 6.205 [7] that gives a total proton-proton cross section of $\sigma_{\text{tot}} = 102.4$ mb, with ≈ 80 mb of inelastic interactions;
- LHC crossing rate = 40.08 MHz;
- number of LHC (filled) bunches = (2622) 3564
- average (instantaneous) luminosity at the LHCb interaction region of $L = 2{\times}10^{32}$ cm^{-2}s^{-1}.

Given these assumptions, we can calculate the rate with at least one interaction:

$$R_{>0} = P_{>0} \times R_{\text{filled}} \quad . \tag{2}$$

$P_{>0}$ is the probability of having at least one interaction in the crossing, and R_{filled} is the frequency of filled bunch crossings at the LHCb interaction point. We have:

- rate of filled bunch crossings at the LHCb interaction point
  $R_{\text{filled}} = 40.08 \times (2622/3564) = 29.49$ MHz;

- average number of interactions in R_{filled} MHz
  $\bar{N}_{\text{int}} = L \times \sigma_{\text{tot}}/R_{\text{filled}} = 0.694$;

- $P_{>0} = 1 - e^{\bar{N}_{\text{int}}} = 0.495$;

- $R_{>0} = 0.495 \times 29.49 = 14.842$ MHz.

As a result the retention rate is just $0.0674 = 1.0/14.842$.

5 Discussion of Results

5.1 Bandwidth Division at Nominal Running Conditions

Table 2 contains the list of L0 E_{T} thresholds obtained after the bandwidth division optimization at the nominal L0 output rate of 1.0 MHz [2].

After the global event cuts the L0 output rate is reduced to about 7 MHz (c.f. table 1). With the thresholds obtained after the optimization at 1.0 MHz, this bandwidth division respectively gives for the hadron, electromagnetic (electron, photon and π^0's) and muon (muon and di-muon) triggers an inclusive L0 output rate of about 705, 282 and 161 kHz, after the global event selection; the discriminated list for all sub-triggers is collected in table 3.

In table 4 we collected the exclusive trigger rates: by itself and exclusively, the hadron trigger accounts for over half of the L0 bandwidth – approximately 560 kHz – whereas all other triggers' exclusive contributions are only of the order of a few percent of the total bandwidth.

One can also infer from table 4 the high correlation of several triggers. The table shows the overlapping trigger rates on minimum-bias events at the nominal output rate of 1.0 MHz. For comparison purposes the inclusive rates have been re-displayed at the bottom of the table. Large overlaps exist between the muon triggers, the electromagnetic and hadron triggers, and between the different electromagnetic triggers.

The overlap between triggers is best seen in table 5, which presents the sub-triggers overlap probabilities on minimum-bias events at the nominal output rate of 1.0 MHz. For

---

[2] A slight simplification was done for the optimization at 1.0 MHz by fixing the π^0 triggers thresholds to the values quoted in table 2. A more detailed analysis of these triggers was performed in a dedicated study [8]. We made this choice given that these triggers have a large overlap with the hadron and electromagnetic triggers (see tables 4 and 5) and therefore small losses in efficiency can still be achieved by compensating with the latter triggers.

each column, corresponding to a given sub-trigger that has fired L0, one can read off the frequency of triggering of another sub-trigger.

In about $40-50\%$ of the time the hadron trigger has also fired when an electromagnetic trigger fired L0. And when one of the electromagnetic triggers fired, the probability that another electromagnetic trigger fired is in general in the range $30-50\%$.

Given our L0 operating settings, the efficiencies for a series of channels were determined; they are collected in table 6. Both the $\varepsilon_{\mathrm{L0}}^{channel}$ and $\varepsilon_{\mathrm{L0-max}}^{channel}$ are shown. This bandwidth division results in remarkably small losses compared to what can be obtained if LHCb would dedicate its running to a single channel: the losses in efficiency are rather low for most of the channels, of the order of a few percent, apart from channels with a decay $\mathrm{J}/\psi \to \mathrm{e}^{+}\mathrm{e}^{-}$, which has to compete with $\mathrm{J}/\psi \to \mu^{+}\mu^{-}$ in the relative loss since it addresses the same CKM measurement, and with the hadron trigger for its share of the bandwidth.

Table 7 presents the inclusive contributions to the efficiencies from the three "groups of triggers" – hadronic, electromagnetic and muon triggers – to show correlations between them. The contributions from the electromagnetic calorimeter triggers have been grouped together, since they are rather redundant and their relative contributions depend on the choice of their highly correlated thresholds. It can be inferred that for each channel the expected most relevant trigger component is always the one that indeed contributes to a larger extent to the performance of L0 ($\varepsilon_{\mathrm{L0}}^{channel}$ is redisplayed in table 7 for convenience).

5.2 Sensitivity of L0 to the Output Rate

The sensitivity of L0 to the output rate was studied with the bandwidth division optimizations being done also at 0.5, 0.7 and 0.9 MHz. The resulting E_{T} thresholds and corresponding inclusive rates are summarized in tables 2 and 3, respectively.

The hadron trigger on one hand, and the electromagnetic and muon triggers on the other hand, present strikingly different behaviours as a function of the L0 output rate, as expected: at a high output rate of 1.0 MHz the hadron trigger inclusively takes a major share of the bandwidth, $\approx 70\%$, over twice the bandwidth taken by the other 2 groups of triggers. But as the output rate is decreased the shares become more even. In fact the rates allocated to the electromagnetic and muon triggers remain roughly constant when going from an output rate of 1.0 to 0.5 MHz, whereas the hadron trigger rate drastically decreases by a factor of ≈ 2.5.

For all these settings at 0.5, 0.7 and 0.9 MHz, the L0 efficiencies $\varepsilon_{\mathrm{L0}}^{channel}$ and $\varepsilon_{\mathrm{L0-max}}^{channel}$ for our set of channels are given in tables 8-10. Again most channels present small losses of the order of a few percent, with a tendency for the losses to slightly increase with decreasing L0 output rate – a best compromise becomes more difficult to obtain.

But the hadron trigger-dominated channels are the ones more affected by the L0 output rate, the "muon channels" presenting fairly constant efficiencies – both $\varepsilon_{\mathrm{L0}}^{channel}$ and $\varepsilon_{\mathrm{L0-max}}^{channel}$ – as a function of the output rate. This is best seen in figures 1 and 2.

Figure 1 shows the sensitivity of $\varepsilon_{\mathrm{L0}}^{channel}$ to the L0 output rate, for a few "representative" channels. The values of $\varepsilon_{\mathrm{L0}}^{channel}$ from 0.5–1.0 MHz were again obtained after a combined optimization of L0 – as described above – for each output rate. The values of $\varepsilon_{\mathrm{L0-max}}^{channel}$ at 1.0 MHz are presented on the right-hand side of the figure, indicating how much is lost in efficiency per channel while sharing the bandwidth over all channels in a democratic way.

The evolution of $\varepsilon_{\mathrm{L0-max}}^{channel}$ can be seen in figure 2 for a few channels. Hadronic channels such as $\mathrm{B_d^0} \to \pi^+\pi^-$ suffer most from the L0 output rate, as the hadron trigger threshold varies significantly between 1.0 and 0.5 MHz – by itself the hadron trigger would take a bandwidth of 1.0 MHz with a threshold at ≈ 3.2 GeV. A muon-dominated channel such as $\mathrm{B_s^0} \to \mathrm{J}/\psi(\mu^+\mu^-)\phi(\mathrm{K^+K^-})$ has a different behaviour, since the muon triggers cannot fill up the 1.0 MHz; only at a very low output rate one would start to see a decrease in the efficiency for such channels.

Tables 11 to 13 present also the inclusive contributions from the three groups of triggers. The most striking point is that the inclusive efficiencies still show a rather constant share as a function of the L0 output rate in spite of the variation of the sharing of the inclusive bandwidths given to the hadron, electromagnetic and muon triggers.

Acknowledgements:

This Research has been supported by a Marie Curie Fellowship of the European Community Program "Improving Human Research Potential and the Socio-economic Knowledge Base" under contract number HPMF-CT-2002-01708.

I would like to thank Claire Shepherd-Themistocleous for introducing me to the subject and Hans Dijkstra for regular and very fruitful discussions.

References

[1] The LHCb Collaboration, R. A. Nobrega *et al.*, *LHCb Reoptimized Detector Design and Performance Technical Design Report*, CERN/LHCC 2003-030, LHCb TDR 9, 2003

[2] O. Callot, M. Ferro-Luzzi and P. Perret, *Using the SPD multiplicity in the Level-0 trigger*, LHCb Trigger Note LHCb 2003-022

[3] M. Ferro-Luzzi *et al.*, *Effect of Multiplicity Cuts on the L0 and L1 Triggers*, LHCb Trigger Note LHCb 2003-047

[4] The LHCb Collaboration, S. Amato *et al.*, Technical Proposal, CERN/LHCC-98-4, 1998

[5] E. Rodrigues, LHCb Trigger Note in preparation

[6] MINUIT Function Minimization and Error Analysis, CERN Program Library Long Writeup D506 (1998)

[7] T. Sjöstrand *et al.*, *High-Energy-Physics Event Generation with PYTHIA 6.2*, *Comp. Phys. Comm.* **135** (2001) 238

[8] O. Deschamps, P. Perret, *Implementation and Performance of Level-0 Trigger System for Neutral Pions*, LHCb Trigger Note LHCb 2003-067

Global Event Cuts	Value	M. B. rate (kHz)
Tracks in 2^{nd} vertex	3	6981 ± 17
Pile-Up Multiplicity	112 hits	
SPD Multiplicity	280 hits	
$\sum E_{\mathrm{T}}$	5.0 GeV	

Table 1: List of L0 cuts on the global event variables. The last column gives the inclusive L0 output rate on minimum-bias events after these four global event cuts (the uncertainty is statistical).

Trigger	E_{T} thresholds (GeV)			
	1.0 MHz	0.9 MHz	0.7 MHz	0.5 MHz
hadron	3.60	3.70	4.40	4.90
electron	2.80	3.20	3.20	4.30
photon	2.60	2.90	3.00	3.20
π^0 local	4.50	5.00	∞	∞
π^0 global	4.00	3.90	3.90	3.70
muon	1.10	1.50	1.60	1.70
$\Sigma p_{\mathrm{T}}^{\mu}$	1.30	1.30	1.30	1.50

Table 2: List of L0 thresholds obtained after the combined optimization at the L0 output rates of 1.0, 0.9, 0.7 and 0.5 MHz.

Trigger	Inclusive M. B. rate (kHz)							
	1.0 MHz		0.9 MHz		0.7 MHz		0.5 MHz	
hadron	705 ± 7		658 ± 7		369 ± 5		257 ± 4	
electron	103 ± 3	282 ± 5	71 ± 2	227 ± 4	71 ± 2	210 ± 4	28 ± 1	208 ± 4
photon	126 ± 3		90 ± 3		79 ± 2		68 ± 2	
π^0 local	110 ± 3		79 ± 2		0 ± 0		0 ± 0	
π^0 global	145 ± 3		160 ± 3		160 ± 3		190 ± 4	
muon	110 ± 3	161 ± 3	78 ± 2	145 ± 3	73 ± 2	145 ± 3	66 ± 2	123 ± 3
$\Sigma p_{\mathrm{T}}^{\mu}$	145 ± 3		145 ± 3		145 ± 3		123 ± 3	

Table 3: List of L0 inclusive rates on minimum-bias events corresponding to the L0 thresholds in table 2, after the four global event cuts, at the L0 output rates of 1.0, 0.9, 0.7 and 0.5 MHz. All uncertainties are statistical.

M. B. rate (kHz)	hadron	electron	photon	π^0 local	π^0 global	muon	$\Sigma p_{\mathrm{T}}^{\mu}$
hadron	561	47	50	58	76	27	24
electron		27	11	44	51	4	4
photon			44	43	53	5	4
π^0 local				7	81	6	5
π^0 global					15	7	6
muon						13	93
$\Sigma p_{\mathrm{T}}^{\mu}$							51
Inclusive M. B. rate (kHz)	705	103	126	110	145	110	145

Table 4: Exclusive (diagonal terms) and overlapping (off-diagonal terms) trigger rates on minimum-bias events at the nominal output rate of 1.0 MHz.

Probability (%)	hadron	electron	photon	π^0 local	π^0 global	muon	$\Sigma p_{\mathrm{T}}^{\mu}$
hadron		46	39	53	53	24	17
electron	7		9	40	35	4	3
photon	7	10		39	37	4	3
π^0 local	8	43	34		56	5	4
π^0 global	11	50	42	74		7	5
muon	4	4	4	5	5		64
$\Sigma p_{\mathrm{T}}^{\mu}$	3	4	3	5	5	85	

Table 5: Sub-triggers overlap probability on minimum-bias events at the nominal output rate of 1.0 MHz : each column gives the frequency of triggering of a sub-trigger given that it triggered another sub-trigger (e.g. in 46% of the events where the electron triggered L0 the hadron trigger has also fired).

Decay Channel	$\varepsilon_{\mathrm{L0-max}}$(%)	$\varepsilon_{\mathrm{L0}}$(%)	loss (%)
$\mathrm{B_d^0 \to \overline{D^0}(K^+\pi^-)K^{*0}(K^+\pi^-)}$	54.0 ± 1.4	53.0 ± 1.4	1.9
$\mathrm{B_d^0 \to \overline{D^0}(K^+K^-)K^{*0}(K^+\pi^-)}$	51.6 ± 1.2	50.7 ± 1.2	1.7
$\mathrm{B_d^0 \to D^{*-}(\overline{D^0}\pi^-)\pi^+}$	49.9 ± 1.1	49.0 ± 1.1	1.8
$\mathrm{B_d^0 \to K^{*0}(K^+\pi^-)\gamma}$	77.6 ± 1.0	72.9 ± 1.0	6.1
$\mathrm{B_d^0 \to K^+\pi^-}$	54.7 ± 0.8	54.1 ± 0.8	1.1
$\mathrm{B_d^0 \to J/\psi(e^+e^-)K_S^0(\pi^+\pi^-)}$	69.7 ± 0.9	48.3 ± 1.0	30.7
$\mathrm{B_d^0 \to J/\psi(\mu^+\mu^-)K_S^0(\pi^+\pi^-)}$	93.0 ± 0.4	89.3 ± 0.5	4.0
$\mathrm{B_d^0 \to J/\psi(\mu^+\mu^-)K^{*0}(K^+\pi^-)}$	93.8 ± 0.2	91.1 ± 0.2	2.9
$\mathrm{B_d^0 \to \mu^+\mu^-K^{*0}(K^+\pi^-)}$	95.6 ± 0.6	93.6 ± 0.7	2.1
$\mathrm{B_d^0 \to \pi^+\pi^-}$	54.7 ± 0.4	53.6 ± 0.4	2.0
$\mathrm{B_d^0 \to \pi^+\pi^-\pi^0}$	81.6 ± 1.5	77.2 ± 1.6	5.4
$\mathrm{B_s^0 \to D_s^-(K^+K^-\pi^-)K^+}$	48.2 ± 0.3	47.2 ± 0.3	2.1
$\mathrm{B_s^0 \to D_s^-(K^+K^-\pi^-)\pi^+}$	50.4 ± 0.6	49.4 ± 0.6	2.0
$\mathrm{B_s^0 \to J/\psi(\mu^+\mu^-)\eta(\gamma\gamma)}$	95.8 ± 0.6	92.1 ± 0.8	3.9
$\mathrm{B_s^0 \to J/\psi(e^+e^-)\phi(K^+K^-)}$	67.3 ± 0.5	49.0 ± 0.6	27.2
$\mathrm{B_s^0 \to J/\psi(\mu^+\mu^-)\phi(K^+K^-)}$	93.0 ± 0.1	89.7 ± 0.1	3.5
$\mathrm{B_s^0 \to K^+K^-}$	53.0 ± 0.3	51.8 ± 0.3	2.3
$\mathrm{B_s^0 \to K^-\pi^+}$	58.0 ± 1.1	56.5 ± 1.1	2.6
$\mathrm{B_s^0 \to \eta_c(4\pi, 2K2\pi)\phi(K^+K^-)}$	51.0 ± 2.9	47.0 ± 3.0	7.8
$\mathrm{B_s^0 \to \phi(K^+K^-)\gamma}$	77.4 ± 1.5	69.5 ± 1.5	10.2
$\mathrm{B_s^0 \to \phi(K^+K^-)\phi(K^+K^-)}$	39.1 ± 0.9	38.5 ± 0.9	1.5
$\mathrm{B_u^+ \to J/\psi(\mu^+\mu^-)K^+}$	93.3 ± 0.3	90.3 ± 0.4	3.2
$\mathrm{B_c^+ \to J/\psi(\mu^+\mu^-)\pi^+}$	95.2 ± 0.4	93.1 ± 0.5	2.2

Table 6: L0 efficiencies at the nominal output rate of 1.0 MHz: maximum efficiency after single channel optimization ($\varepsilon_{\mathrm{L0-max}}$); efficiency after combined optimization of the L0 trigger ($\varepsilon_{\mathrm{L0}}$); and loss in efficiency ($(\varepsilon_{\mathrm{L0-max}} - \varepsilon_{\mathrm{L0}})/\varepsilon_{\mathrm{L0-max}}$). All uncertainties are statistical.

Decay Channel	$\varepsilon_{\mathrm{L0}}(\%)$	Inclusive efficiencies (%)		
		had. trig.	elec. trig.	muon trig.
$\mathrm{B^0_d \to \overline{D^0}(K^+\pi^-)K^{*0}(K^+\pi^-)}$	53.0 ± 1.4	45.3 ± 1.4	13.9 ± 0.9	8.1 ± 0.7
$\mathrm{B^0_d \to \overline{D^0}(K^+K^-)K^{*0}(K^+\pi^-)}$	50.7 ± 1.2	43.4 ± 1.2	13.6 ± 0.8	8.4 ± 0.7
$\mathrm{B^0_d \to D^{*-}(\overline{D^0}\pi^-)\pi^+}$	49.0 ± 1.1	41.7 ± 1.1	14.0 ± 0.8	8.4 ± 0.6
$\mathrm{B^0_d \to K^{*0}(K^+\pi^-)\gamma}$	72.9 ± 1.0	32.7 ± 1.1	68.1 ± 1.1	7.8 ± 0.6
$\mathrm{B^0_d \to K^+\pi^-}$	54.1 ± 0.8	48.3 ± 0.8	12.3 ± 0.5	7.2 ± 0.4
$\mathrm{B^0_d \to J/\psi(e^+e^-)K^0_S(\pi^+\pi^-)}$	48.3 ± 1.0	21.5 ± 0.8	37.4 ± 0.9	7.0 ± 0.5
$\mathrm{B^0_d \to J/\psi(\mu^+\mu^-)K^0_S(\pi^+\pi^-)}$	89.3 ± 0.5	18.6 ± 0.7	8.3 ± 0.5	87.2 ± 0.6
$\mathrm{B^0_d \to J/\psi(\mu^+\mu^-)K^{*0}(K^+\pi^-)}$	91.1 ± 0.2	23.1 ± 0.4	9.3 ± 0.3	88.6 ± 0.3
$\mathrm{B^0_d \to \mu^+\mu^-K^{*0}(K^+\pi^-)}$	93.6 ± 0.7	24.9 ± 1.2	10.3 ± 0.8	91.8 ± 0.7
$\mathrm{B^0_d \to \pi^+\pi^-}$	53.6 ± 0.4	47.6 ± 0.5	14.1 ± 0.3	6.8 ± 0.2
$\mathrm{B^0_d \to \pi^+\pi^-\pi^0}$	77.2 ± 1.6	39.4 ± 1.9	66.2 ± 1.8	7.9 ± 1.1
$\mathrm{B^0_s \to D^-_s(K^+K^-\pi^-)K^+}$	47.2 ± 0.3	39.4 ± 0.3	11.7 ± 0.2	8.2 ± 0.2
$\mathrm{B^0_s \to D^-_s(K^+K^-\pi^-)\pi^+}$	49.4 ± 0.6	42.2 ± 0.6	13.1 ± 0.4	8.3 ± 0.4
$\mathrm{B^0_s \to J/\psi(\mu^+\mu^-)\eta(\gamma\gamma)}$	92.1 ± 0.8	19.2 ± 1.2	37.2 ± 1.5	88.4 ± 1.0
$\mathrm{B^0_s \to J/\psi(e^+e^-)\phi(K^+K^-)}$	49.0 ± 0.6	22.9 ± 0.5	38.3 ± 0.5	7.0 ± 0.3
$\mathrm{B^0_s \to J/\psi(\mu^+\mu^-)\phi(K^+K^-)}$	89.7 ± 0.1	20.0 ± 0.2	8.4 ± 0.1	87.4 ± 0.1
$\mathrm{B^0_s \to K^+K^-}$	51.8 ± 0.3	46.0 ± 0.3	11.6 ± 0.2	6.5 ± 0.2
$\mathrm{B^0_s \to K^-\pi^+}$	56.5 ± 1.1	51.2 ± 1.1	13.2 ± 0.7	6.7 ± 0.5
$\mathrm{B^0_s \to \eta_c(4\pi, 2K2\pi)\phi(K^+K^-)}$	47.0 ± 3.0	41.5 ± 2.9	12.5 ± 1.9	8.0 ± 1.6
$\mathrm{B^0_s \to \phi(K^+K^-)\gamma}$	69.5 ± 1.5	33.1 ± 1.6	65.8 ± 1.7	7.7 ± 0.9
$\mathrm{B^0_s \to \phi(K^+K^-)\phi(K^+K^-)}$	38.5 ± 0.9	28.7 ± 0.9	9.7 ± 0.6	8.6 ± 0.5
$\mathrm{B^+_u \to J/\psi(\mu^+\mu^-)K^+}$	90.3 ± 0.4	26.2 ± 0.5	9.1 ± 0.4	87.1 ± 0.4
$\mathrm{B^+_c \to J/\psi(\mu^+\mu^-)\pi^+}$	93.1 ± 0.5	29.4 ± 0.8	9.9 ± 0.5	89.5 ± 0.6

Table 7: L0 inclusive efficiencies at 1.0 MHz for the hadronic, electromagnetic (electron, photon, π^0's) and muon triggers. These were obtained after the optimization of the L0 trigger, with the resulting efficiencies being reshown (for easy reference) in the second column. All uncertainties are statistical.

Decay Channel	$\varepsilon_{\mathrm{L0-max}}(\%)$	$\varepsilon_{\mathrm{L0}}(\%)$	loss (%)
$\mathrm{B_d^0} \to \overline{\mathrm{D^0}}(\mathrm{K^+}\pi^-)\mathrm{K^{*0}}(\mathrm{K^+}\pi^-)$	48.3 ± 1.4	46.8 ± 1.4	3.1
$\mathrm{B_d^0} \to \overline{\mathrm{D^0}}(\mathrm{K^+K^-})\mathrm{K^{*0}}(\mathrm{K^+}\pi^-)$	47.2 ± 1.2	46.5 ± 1.2	1.5
$\mathrm{B_d^0} \to \mathrm{D^{*-}}(\overline{\mathrm{D^0}}\pi^-)\pi^+$	47.5 ± 1.1	46.9 ± 1.1	1.3
$\mathrm{B_d^0} \to \mathrm{K^{*0}}(\mathrm{K^+}\pi^-)\gamma$	75.3 ± 1.0	71.8 ± 1.1	4.6
$\mathrm{B_d^0} \to \mathrm{K^+}\pi^-$	52.8 ± 0.8	52.2 ± 0.8	1.1
$\mathrm{B_d^0} \to \mathrm{J}/\psi(\mathrm{e^+e^-})\mathrm{K_S^0}(\pi^+\pi^-)$	68.2 ± 0.9	43.8 ± 1.0	35.8
$\mathrm{B_d^0} \to \mathrm{J}/\psi(\mu^+\mu^-)\mathrm{K_S^0}(\pi^+\pi^-)$	92.8 ± 0.5	88.4 ± 0.6	4.7
$\mathrm{B_d^0} \to \mathrm{J}/\psi(\mu^+\mu^-)\mathrm{K^{*0}}(\mathrm{K^+}\pi^-)$	93.6 ± 0.2	90.0 ± 0.3	3.9
$\mathrm{B_d^0} \to \mu^+\mu^-\mathrm{K^{*0}}(\mathrm{K^+}\pi^-)$	95.7 ± 0.5	92.3 ± 0.7	3.6
$\mathrm{B_d^0} \to \pi^+\pi^-$	52.4 ± 0.4	51.9 ± 0.5	1.0
$\mathrm{B_d^0} \to \pi^+\pi^-\pi^0$	80.4 ± 1.5	74.0 ± 1.7	8.0
$\mathrm{B_s^0} \to \mathrm{D_s^-}(\mathrm{K^+K^-}\pi^-)\mathrm{K^+}$	45.3 ± 0.3	45.0 ± 0.3	0.7
$\mathrm{B_s^0} \to \mathrm{D_s^-}(\mathrm{K^+K^-}\pi^-)\pi^+$	47.5 ± 0.6	47.4 ± 0.6	0.2
$\mathrm{B_s^0} \to \mathrm{J}/\psi(\mu^+\mu^-)\eta(\gamma\gamma)$	95.5 ± 0.7	91.6 ± 0.9	4.1
$\mathrm{B_s^0} \to \mathrm{J}/\psi(\mathrm{e^+e^-})\phi(\mathrm{K^+K^-})$	66.1 ± 0.5	44.6 ± 0.6	32.5
$\mathrm{B_s^0} \to \mathrm{J}/\psi(\mu^+\mu^-)\phi(\mathrm{K^+K^-})$	92.8 ± 0.1	88.4 ± 0.1	4.7
$\mathrm{B_s^0} \to \mathrm{K^+K^-}$	51.1 ± 0.3	50.2 ± 0.3	1.8
$\mathrm{B_s^0} \to \mathrm{K^-}\pi^+$	55.8 ± 1.1	54.9 ± 1.1	1.6
$\mathrm{B_s^0} \to \eta_{\mathrm{c}}(4\pi, 2\mathrm{K}2\pi)\phi(\mathrm{K^+K^-})$	49.5 ± 2.9	45.7 ± 2.9	7.7
$\mathrm{B_s^0} \to \phi(\mathrm{K^+K^-})\gamma$	74.6 ± 1.5	69.6 ± 1.6	6.7
$\mathrm{B_s^0} \to \phi(\mathrm{K^+K^-})\phi(\mathrm{K^+K^-})$	36.9 ± 0.9	35.1 ± 0.9	4.9
$\mathrm{B_u^+} \to \mathrm{J}/\psi(\mu^+\mu^-)\mathrm{K^+}$	93.1 ± 0.3	89.1 ± 0.4	4.3
$\mathrm{B_c^+} \to \mathrm{J}/\psi(\mu^+\mu^-)\pi^+$	95.1 ± 0.4	92.2 ± 0.5	3.0

Table 8: L0 efficiencies at the output rate of 0.9 MHz: maximum efficiency after single channel optimization ($\varepsilon_{\mathrm{L0-max}}$); efficiency after combined optimization of the L0 trigger ($\varepsilon_{\mathrm{L0}}$); and loss in efficiency ($(\varepsilon_{\mathrm{L0-max}}-\varepsilon_{\mathrm{L0}})/\varepsilon_{\mathrm{L0-max}}$). All uncertainties are statistical.

Decay Channel	$\varepsilon_{\mathrm{L0-max}}(\%)$	$\varepsilon_{\mathrm{L0}}(\%)$	loss (%)
$\mathrm{B_d^0} \to \overline{\mathrm{D^0}}(\mathrm{K^+}\pi^-)\mathrm{K^{*0}}(\mathrm{K^+}\pi^-)$	43.3 ± 1.4	37.6 ± 1.4	13.2
$\mathrm{B_d^0} \to \overline{\mathrm{D^0}}(\mathrm{K^+K^-})\mathrm{K^{*0}}(\mathrm{K^+}\pi^-)$	41.4 ± 1.2	38.1 ± 1.2	8.0
$\mathrm{B_d^0} \to \mathrm{D^{*-}}(\overline{\mathrm{D^0}}\pi^-)\pi^+$	40.3 ± 1.1	38.6 ± 1.1	4.2
$\mathrm{B_d^0} \to \mathrm{K^{*0}}(\mathrm{K^+}\pi^-)\gamma$	74.9 ± 1.0	70.1 ± 1.1	6.4
$\mathrm{B_d^0} \to \mathrm{K^+}\pi^-$	46.6 ± 0.8	42.6 ± 0.8	8.6
$\mathrm{B_d^0} \to \mathrm{J}/\psi(\mathrm{e^+e^-})\mathrm{K_S^0}(\pi^+\pi^-)$	64.9 ± 0.9	39.6 ± 1.0	39.0
$\mathrm{B_d^0} \to \mathrm{J}/\psi(\mu^+\mu^-)\mathrm{K_S^0}(\pi^+\pi^-)$	92.3 ± 0.5	87.6 ± 0.6	5.1
$\mathrm{B_d^0} \to \mathrm{J}/\psi(\mu^+\mu^-)\mathrm{K^{*0}}(\mathrm{K^+}\pi^-)$	93.2 ± 0.3	89.1 ± 0.3	4.4
$\mathrm{B_d^0} \to \mu^+\mu^-\mathrm{K^{*0}}(\mathrm{K^+}\pi^-)$	95.3 ± 0.6	91.3 ± 0.8	4.2
$\mathrm{B_d^0} \to \pi^+\pi^-$	46.6 ± 0.4	42.4 ± 0.4	9.0
$\mathrm{B_d^0} \to \pi^+\pi^-\pi^0$	78.5 ± 1.6	70.5 ± 1.8	10.2
$\mathrm{B_s^0} \to \mathrm{D_s^-}(\mathrm{K^+K^-}\pi^-)\mathrm{K^+}$	38.1 ± 0.3	35.7 ± 0.3	6.3
$\mathrm{B_s^0} \to \mathrm{D_s^-}(\mathrm{K^+K^-}\pi^-)\pi^+$	41.4 ± 0.6	38.6 ± 0.6	6.8
$\mathrm{B_s^0} \to \mathrm{J}/\psi(\mu^+\mu^-)\eta(\gamma\gamma)$	93.6 ± 0.8	91.1 ± 0.9	2.7
$\mathrm{B_s^0} \to \mathrm{J}/\psi(\mathrm{e^+e^-})\phi(\mathrm{K^+K^-})$	63.5 ± 0.5	40.3 ± 0.6	36.5
$\mathrm{B_s^0} \to \mathrm{J}/\psi(\mu^+\mu^-)\phi(\mathrm{K^+K^-})$	92.3 ± 0.1	87.5 ± 0.1	5.2
$\mathrm{B_s^0} \to \mathrm{K^+K^-}$	44.3 ± 0.3	40.3 ± 0.3	9.0
$\mathrm{B_s^0} \to \mathrm{K^-}\pi^+$	50.1 ± 1.1	44.1 ± 1.1	12.0
$\mathrm{B_s^0} \to \eta_\mathrm{c}(4\pi, 2\mathrm{K}2\pi)\phi(\mathrm{K^+K^-})$	42.6 ± 2.9	38.4 ± 2.9	9.9
$\mathrm{B_s^0} \to \phi(\mathrm{K^+K^-})\gamma$	73.9 ± 1.5	67.6 ± 1.6	8.5
$\mathrm{B_s^0} \to \phi(\mathrm{K^+K^-})\phi(\mathrm{K^+K^-})$	29.8 ± 0.9	26.6 ± 0.8	10.7
$\mathrm{B_u^+} \to \mathrm{J}/\psi(\mu^+\mu^-)\mathrm{K^+}$	92.6 ± 0.3	87.9 ± 0.4	5.1
$\mathrm{B_c^+} \to \mathrm{J}/\psi(\mu^+\mu^-)\pi^+$	94.4 ± 0.4	91.3 ± 0.5	3.3

Table 9: L0 efficiencies at the output rate of 0.7 MHz: maximum efficiency after single channel optimization ($\varepsilon_{\mathrm{L0-max}}$); efficiency after combined optimization of the L0 trigger ($\varepsilon_{\mathrm{L0}}$); and loss in efficiency $((\varepsilon_{\mathrm{L0-max}} - \varepsilon_{\mathrm{L0}})/\varepsilon_{\mathrm{L0-max}})$. All uncertainties are statistical.

Decay Channel	$\varepsilon_{\mathrm{L0-max}}(\%)$	$\varepsilon_{\mathrm{L0}}(\%)$	loss (%)
$\mathrm{B_d^0} \to \overline{\mathrm{D}^0}(\mathrm{K}^+\pi^-)\mathrm{K}^{*0}(\mathrm{K}^+\pi^-)$	36.0 ± 1.4	32.1 ± 1.3	10.8
$\mathrm{B_d^0} \to \overline{\mathrm{D}^0}(\mathrm{K}^+\mathrm{K}^-)\mathrm{K}^{*0}(\mathrm{K}^+\pi^-)$	35.2 ± 1.1	32.4 ± 1.1	8.0
$\mathrm{B_d^0} \to \mathrm{D}^{*-}(\overline{\mathrm{D}^0}\pi^-)\pi^+$	34.9 ± 1.1	33.5 ± 1.1	4.0
$\mathrm{B_d^0} \to \mathrm{K}^{*0}(\mathrm{K}^+\pi^-)\gamma$	72.2 ± 1.1	66.2 ± 1.1	8.3
$\mathrm{B_d^0} \to \mathrm{K}^+\pi^-$	40.9 ± 0.8	37.1 ± 0.8	9.3
$\mathrm{B_d^0} \to \mathrm{J}/\psi(\mathrm{e}^+\mathrm{e}^-)\mathrm{K_S^0}(\pi^+\pi^-)$	60.6 ± 1.0	33.8 ± 0.9	44.2
$\mathrm{B_d^0} \to \mathrm{J}/\psi(\mu^+\mu^-)\mathrm{K_S^0}(\pi^+\pi^-)$	92.1 ± 0.5	84.8 ± 0.6	7.9
$\mathrm{B_d^0} \to \mathrm{J}/\psi(\mu^+\mu^-)\mathrm{K}^{*0}(\mathrm{K}^+\pi^-)$	92.6 ± 0.3	87.0 ± 0.3	6.0
$\mathrm{B_d^0} \to \mu^+\mu^-\mathrm{K}^{*0}(\mathrm{K}^+\pi^-)$	95.0 ± 0.6	89.4 ± 0.8	5.9
$\mathrm{B_d^0} \to \pi^+\pi^-$	40.9 ± 0.4	36.2 ± 0.4	11.5
$\mathrm{B_d^0} \to \pi^+\pi^-\pi^0$	74.5 ± 1.7	68.3 ± 1.8	8.3
$\mathrm{B_s^0} \to \mathrm{D_s^-}(\mathrm{K}^+\mathrm{K}^-\pi^-)\mathrm{K}^+$	32.9 ± 0.3	30.4 ± 0.3	7.6
$\mathrm{B_s^0} \to \mathrm{D_s^-}(\mathrm{K}^+\mathrm{K}^-\pi^-)\pi^+$	34.8 ± 0.6	33.6 ± 0.6	3.5
$\mathrm{B_s^0} \to \mathrm{J}/\psi(\mu^+\mu^-)\eta(\gamma\gamma)$	93.9 ± 0.8	89.9 ± 0.9	4.3
$\mathrm{B_s^0} \to \mathrm{J}/\psi(\mathrm{e}^+\mathrm{e}^-)\phi(\mathrm{K}^+\mathrm{K}^-)$	56.6 ± 0.6	35.2 ± 0.5	37.8
$\mathrm{B_s^0} \to \mathrm{J}/\psi(\mu^+\mu^-)\phi(\mathrm{K}^+\mathrm{K}^-)$	91.7 ± 0.1	84.8 ± 0.2	7.5
$\mathrm{B_s^0} \to \mathrm{K}^+\mathrm{K}^-$	38.9 ± 0.3	34.3 ± 0.3	11.8
$\mathrm{B_s^0} \to \mathrm{K}^-\pi^+$	44.2 ± 1.1	37.5 ± 1.1	15.2
$\mathrm{B_s^0} \to \eta_\mathrm{c}(4\pi, 2\mathrm{K}2\pi)\phi(\mathrm{K}^+\mathrm{K}^-)$	37.4 ± 2.9	35.3 ± 2.8	5.6
$\mathrm{B_s^0} \to \phi(\mathrm{K}^+\mathrm{K}^-)\gamma$	71.2 ± 1.6	64.7 ± 1.7	9.1
$\mathrm{B_s^0} \to \phi(\mathrm{K}^+\mathrm{K}^-)\phi(\mathrm{K}^+\mathrm{K}^-)$	23.5 ± 0.8	22.7 ± 0.8	3.4
$\mathrm{B_u^+} \to \mathrm{J}/\psi(\mu^+\mu^-)\mathrm{K}^+$	91.2 ± 0.3	85.2 ± 0.4	6.6
$\mathrm{B_c^+} \to \mathrm{J}/\psi(\mu^+\mu^-)\pi^+$	93.5 ± 0.4	89.0 ± 0.6	4.8

Table 10: L0 efficiencies at the output rate of 0.5 MHz: maximum efficiency after single channel optimization ($\varepsilon_{\mathrm{L0-max}}$); efficiency after combined optimization of the L0 trigger ($\varepsilon_{\mathrm{L0}}$); and loss in efficiency ($(\varepsilon_{\mathrm{L0-max}} - \varepsilon_{\mathrm{L0}})/\varepsilon_{\mathrm{L0-max}}$). All uncertainties are statistical.

Decay Channel	$\varepsilon_{\mathrm{L0}}(\%)$	Inclusive efficiencies (%)		
		had. trig.	elec. trig.	muon trig.
$B_d^0 \to \overline{D^0}(K^+\pi^-)K^{*0}(K^+\pi^-)$	46.8 ± 1.4	40.4 ± 1.4	10.8 ± 0.9	7.1 ± 0.7
$B_d^0 \to \overline{D^0}(K^+K^-)K^{*0}(K^+\pi^-)$	46.5 ± 1.2	40.0 ± 1.2	11.4 ± 0.8	7.6 ± 0.6
$B_d^0 \to D^{*-}(\overline{D^0}\pi^-)\pi^+$	46.9 ± 1.1	39.9 ± 1.1	12.2 ± 0.7	7.9 ± 0.6
$B_d^0 \to K^{*0}(K^+\pi^-)\gamma$	71.8 ± 1.1	31.3 ± 0.8	66.5 ± 1.1	7.3 ± 0.6
$B_d^0 \to K^+\pi^-$	52.2 ± 0.8	47.0 ± 0.8	10.9 ± 0.5	6.4 ± 0.4
$B_d^0 \to J/\psi(e^+e^-)K_S^0(\pi^+\pi^-)$	43.8 ± 1.0	20.4 ± 0.8	31.9 ± 0.9	6.6 ± 0.5
$B_d^0 \to J/\psi(\mu^+\mu^-)K_S^0(\pi^+\pi^-)$	88.4 ± 0.6	17.6 ± 0.7	6.9 ± 0.4	86.0 ± 0.6
$B_d^0 \to J/\psi(\mu^+\mu^-)K^{*0}(K^+\pi^-)$	90.0 ± 0.3	22.0 ± 0.4	8.0 ± 0.3	87.4 ± 0.3
$B_d^0 \to \mu^+\mu^-K^{*0}(K^+\pi^-)$	92.3 ± 0.7	24.0 ± 1.0	9.6 ± 0.8	90.1 ± 0.8
$B_d^0 \to \pi^+\pi^-$	51.9 ± 0.5	46.3 ± 0.5	12.4 ± 0.3	6.3 ± 0.2
$B_d^0 \to \pi^+\pi^-\pi^0$	74.0 ± 1.7	38.6 ± 1.9	63.5 ± 1.9	7.5 ± 1.0
$B_s^0 \to D_s^-(K^+K^-\pi^-)K^+$	45.0 ± 0.3	38.0 ± 0.3	10.2 ± 0.2	7.6 ± 0.2
$B_s^0 \to D_s^-(K^+K^-\pi^-)\pi^+$	47.4 ± 0.6	40.8 ± 0.6	11.7 ± 0.4	7.4 ± 0.3
$B_s^0 \to J/\psi(\mu^+\mu^-)\eta(\gamma\gamma)$	91.6 ± 0.9	18.3 ± 1.2	33.7 ± 1.5	87.2 ± 1.0
$B_s^0 \to J/\psi(e^+e^-)\phi(K^+K^-)$	44.6 ± 0.6	21.8 ± 0.5	32.9 ± 0.5	6.4 ± 0.3
$B_s^0 \to J/\psi(\mu^+\mu^-)\phi(K^+K^-)$	88.4 ± 0.1	18.9 ± 0.2	7.2 ± 0.1	85.9 ± 0.2
$B_s^0 \to K^+K^-$	50.2 ± 0.3	44.5 ± 0.3	10.3 ± 0.2	6.0 ± 0.1
$B_s^0 \to K^-\pi^+$	54.9 ± 1.1	49.8 ± 1.1	12.2 ± 0.7	5.9 ± 0.5
$B_s^0 \to \eta_c(4\pi, 2K2\pi)\phi(K^+K^-)$	45.7 ± 2.9	40.1 ± 2.9	11.8 ± 1.9	7.3 ± 1.5
$B_s^0 \to \phi(K^+K^-)\gamma$	69.6 ± 1.6	31.9 ± 1.6	64.6 ± 1.7	6.7 ± 0.9
$B_s^0 \to \phi(K^+K^-)\phi(K^+K^-)$	35.1 ± 0.9	27.1 ± 0.8	7.9 ± 0.5	7.5 ± 0.5
$B_u^+ \to J/\psi(\mu^+\mu^-)K^+$	89.1 ± 0.4	25.3 ± 0.5	7.6 ± 0.3	85.6 ± 0.4
$B_c^+ \to J/\psi(\mu^+\mu^-)\pi^+$	92.2 ± 0.5	28.0 ± 0.8	8.5 ± 0.5	88.3 ± 0.6

Table 11: L0 inclusive efficiencies at 0.9 MHz for the hadronic, electromagnetic (electron, photon, π^0's) and muon triggers. These were obtained after the optimization of the L0 trigger, with the resulting efficiencies being reshown (for easy reference) in the second column. All uncertainties are statistical.

Decay Channel	$\varepsilon_{\mathrm{L0}}(\%)$	Inclusive efficiencies (%)		
		had. trig.	elec. trig.	muon trig.
$\mathrm{B_d^0} \to \overline{\mathrm{D^0}}(\mathrm{K^+}\pi^-)\mathrm{K^{*0}}(\mathrm{K^+}\pi^-)$	37.6 ± 1.4	29.8 ± 1.3	9.7 ± 0.8	7.1 ± 0.7
$\mathrm{B_d^0} \to \overline{\mathrm{D^0}}(\mathrm{K^+K^-})\mathrm{K^{*0}}(\mathrm{K^+}\pi^-)$	38.1 ± 1.2	29.5 ± 1.1	10.9 ± 0.7	7.6 ± 0.6
$\mathrm{B_d^0} \to \mathrm{D^{*-}}(\overline{\mathrm{D^0}}\pi^-)\pi^+$	38.6 ± 1.1	30.5 ± 1.1	11.7 ± 0.7	7.9 ± 0.6
$\mathrm{B_d^0} \to \mathrm{K^{*0}}(\mathrm{K^+}\pi^-)\gamma$	70.1 ± 1.1	23.0 ± 1.0	65.5 ± 1.1	7.3 ± 0.6
$\mathrm{B_d^0} \to \mathrm{K^+}\pi^-$	42.6 ± 0.8	35.8 ± 0.8	10.5 ± 0.5	6.4 ± 0.4
$\mathrm{B_d^0} \to \mathrm{J}/\psi(\mathrm{e^+e^-})\mathrm{K_S^0}(\pi^+\pi^-)$	39.6 ± 1.0	13.2 ± 0.7	31.4 ± 0.9	6.6 ± 0.5
$\mathrm{B_d^0} \to \mathrm{J}/\psi(\mu^+\mu^-)\mathrm{K_S^0}(\pi^+\pi^-)$	87.6 ± 0.6	11.1 ± 0.6	6.4 ± 0.4	86.0 ± 0.6
$\mathrm{B_d^0} \to \mathrm{J}/\psi(\mu^+\mu^-)\mathrm{K^{*0}}(\mathrm{K^+}\pi^-)$	89.1 ± 0.3	14.3 ± 0.3	7.5 ± 0.3	87.4 ± 0.3
$\mathrm{B_d^0} \to \mu^+\mu^-\mathrm{K^{*0}}(\mathrm{K^+}\pi^-)$	91.3 ± 0.8	15.8 ± 1.0	9.0 ± 0.8	90.1 ± 0.8
$\mathrm{B_d^0} \to \pi^+\pi^-$	42.4 ± 0.4	35.2 ± 0.4	11.8 ± 0.3	6.3 ± 0.2
$\mathrm{B_d^0} \to \pi^+\pi^-\pi^0$	70.5 ± 1.8	29.8 ± 1.8	62.7 ± 1.9	7.5 ± 1.0
$\mathrm{B_s^0} \to \mathrm{D_s^-}(\mathrm{K^+K^-}\pi^-)\mathrm{K^+}$	35.7 ± 0.3	27.2 ± 0.3	9.7 ± 0.2	7.6 ± 0.2
$\mathrm{B_s^0} \to \mathrm{D_s^-}(\mathrm{K^+K^-}\pi^-)\pi^+$	38.6 ± 0.6	30.5 ± 0.6	11.3 ± 0.4	7.4 ± 0.3
$\mathrm{B_s^0} \to \mathrm{J}/\psi(\mu^+\mu^-)\eta(\gamma\gamma)$	91.1 ± 0.9	13.2 ± 1.1	32.3 ± 1.5	87.2 ± 1.0
$\mathrm{B_s^0} \to \mathrm{J}/\psi(\mathrm{e^+e^-})\phi(\mathrm{K^+K^-})$	40.3 ± 0.6	14.0 ± 0.4	32.2 ± 0.5	6.4 ± 0.3
$\mathrm{B_s^0} \to \mathrm{J}/\psi(\mu^+\mu^-)\phi(\mathrm{K^+K^-})$	87.5 ± 0.1	12.0 ± 0.1	6.7 ± 0.1	85.9 ± 0.2
$\mathrm{B_s^0} \to \mathrm{K^+K^-}$	40.3 ± 0.3	33.3 ± 0.3	9.9 ± 0.2	6.0 ± 0.1
$\mathrm{B_s^0} \to \mathrm{K^-}\pi^+$	44.1 ± 1.1	37.9 ± 1.1	12.1 ± 0.7	5.9 ± 0.5
$\mathrm{B_s^0} \to \eta_c(4\pi, 2\mathrm{K}2\pi)\phi(\mathrm{K^+K^-})$	38.4 ± 2.9	30.5 ± 2.7	10.7 ± 1.8	7.3 ± 1.5
$\mathrm{B_s^0} \to \phi(\mathrm{K^+K^-})\gamma$	67.6 ± 1.6	23.0 ± 1.5	63.4 ± 1.7	6.7 ± 0.9
$\mathrm{B_s^0} \to \phi(\mathrm{K^+K^-})\phi(\mathrm{K^+K^-})$	26.6 ± 0.8	17.3 ± 0.7	7.5 ± 0.5	7.5 ± 0.5
$\mathrm{B_u^+} \to \mathrm{J}/\psi(\mu^+\mu^-)\mathrm{K^+}$	87.9 ± 0.4	16.6 ± 0.5	7.2 ± 0.3	85.6 ± 0.4
$\mathrm{B_c^+} \to \mathrm{J}/\psi(\mu^+\mu^-)\pi^+$	91.3 ± 0.5	19.5 ± 0.7	8.1 ± 0.5	88.3 ± 0.6

Table 12: L0 inclusive efficiencies at 0.7 MHz for the hadronic, electromagnetic (electron, photon, π^0's) and muon triggers. These were obtained after the optimization of the L0 trigger, with the resulting efficiencies being reshown (for easy reference) in the second column. All uncertainties are statistical.

Decay Channel	$\varepsilon_{\mathrm{L0}}(\%)$	Inclusive efficiencies (%)		
		had. trig.	elec. trig.	muon trig.
$\mathrm{B_d^0} \to \overline{\mathrm{D^0}}(\mathrm{K^+}\pi^-)\mathrm{K^{*0}}(\mathrm{K^+}\pi^-)$	32.1 ± 1.3	23.5 ± 1.2	9.3 ± 0.8	6.3 ± 0.7
$\mathrm{B_d^0} \to \overline{\mathrm{D^0}}(\mathrm{K^+K^-})\mathrm{K^{*0}}(\mathrm{K^+}\pi^-)$	32.4 ± 1.1	22.6 ± 1.0	10.4 ± 0.7	6.6 ± 0.6
$\mathrm{B_d^0} \to \mathrm{D^{*-}}(\overline{\mathrm{D^0}}\pi^-)\pi^+$	33.5 ± 1.1	24.3 ± 1.0	11.2 ± 0.7	6.9 ± 0.6
$\mathrm{B_d^0} \to \mathrm{K^{*0}}(\mathrm{K^+}\pi^-)\gamma$	66.2 ± 1.1	18.2 ± 0.9	60.3 ± 1.2	6.5 ± 0.6
$\mathrm{B_d^0} \to \mathrm{K^+}\pi^-$	37.1 ± 0.8	28.6 ± 0.7	10.3 ± 0.5	5.6 ± 0.4
$\mathrm{B_d^0} \to \mathrm{J}/\psi(\mathrm{e^+e^-})\mathrm{K_S^0}(\pi^+\pi^-)$	33.8 ± 0.9	10.1 ± 0.6	26.2 ± 0.9	5.6 ± 0.5
$\mathrm{B_d^0} \to \mathrm{J}/\psi(\mu^+\mu^-)\mathrm{K_S^0}(\pi^+\pi^-)$	84.8 ± 0.6	8.5 ± 0.5	6.1 ± 0.4	81.1 ± 0.7
$\mathrm{B_d^0} \to \mathrm{J}/\psi(\mu^+\mu^-)\mathrm{K^{*0}}(\mathrm{K^+}\pi^-)$	87.0 ± 0.3	10.3 ± 0.3	7.4 ± 0.3	83.2 ± 0.3
$\mathrm{B_d^0} \to \mu^+\mu^-\mathrm{K^{*0}}(\mathrm{K^+}\pi^-)$	89.4 ± 0.8	12.1 ± 0.9	8.9 ± 0.8	85.6 ± 0.9
$\mathrm{B_d^0} \to \pi^+\pi^-$	36.2 ± 0.4	27.6 ± 0.4	11.7 ± 0.3	5.3 ± 0.2
$\mathrm{B_d^0} \to \pi^+\pi^-\pi^0$	68.3 ± 1.8	25.4 ± 1.7	60.7 ± 1.9	6.9 ± 1.0
$\mathrm{B_s^0} \to \mathrm{D_s^-}(\mathrm{K^+K^-}\pi^-)\mathrm{K^+}$	30.4 ± 0.3	20.8 ± 0.2	9.4 ± 0.2	6.6 ± 0.2
$\mathrm{B_s^0} \to \mathrm{D_s^-}(\mathrm{K^+K^-}\pi^-)\pi^+$	33.6 ± 0.6	24.4 ± 0.6	11.1 ± 0.4	6.6 ± 0.3
$\mathrm{B_s^0} \to \mathrm{J}/\psi(\mu^+\mu^-)\eta(\gamma\gamma)$	89.9 ± 0.9	10.0 ± 0.9	30.4 ± 1.4	83.3 ± 1.2
$\mathrm{B_s^0} \to \mathrm{J}/\psi(\mathrm{e^+e^-})\phi(\mathrm{K^+K^-})$	35.2 ± 0.5	10.0 ± 0.3	27.9 ± 0.5	5.5 ± 0.3
$\mathrm{B_s^0} \to \mathrm{J}/\psi(\mu^+\mu^-)\phi(\mathrm{K^+K^-})$	84.8 ± 0.2	8.5 ± 0.1	6.5 ± 0.1	81.1 ± 0.2
$\mathrm{B_s^0} \to \mathrm{K^+K^-}$	34.3 ± 0.3	26.2 ± 0.3	9.7 ± 0.2	5.2 ± 0.1
$\mathrm{B_s^0} \to \mathrm{K^-}\pi^+$	37.5 ± 1.1	29.4 ± 1.0	11.4 ± 0.7	5.4 ± 0.5
$\mathrm{B_s^0} \to \eta_{\mathrm{c}}(4\mathrm{K}, 4\pi, 2\mathrm{K}2\pi)\phi(\mathrm{K^+K^-})$	35.3 ± 2.8	25.6 ± 2.6	11.1 ± 1.9	5.7 ± 1.4
$\mathrm{B_s^0} \to \phi(\mathrm{K^+K^-})\gamma$	64.7 ± 1.7	18.6 ± 1.4	58.9 ± 1.7	5.8 ± 0.8
$\mathrm{B_s^0} \to \phi(\mathrm{K^+K^-})\phi(\mathrm{K^+K^-})$	22.7 ± 0.8	13.0 ± 0.6	7.5 ± 0.5	6.3 ± 0.5
$\mathrm{B_u^+} \to \mathrm{J}/\psi(\mu^+\mu^-)\mathrm{K^+}$	85.2 ± 0.4	12.0 ± 0.4	7.0 ± 0.3	81.1 ± 0.5
$\mathrm{B_c^+} \to \mathrm{J}/\psi(\mu^+\mu^-)\pi^+$	89.0 ± 0.6	15.1 ± 0.6	7.8 ± 0.5	83.7 ± 0.7

Table 13: L0 inclusive efficiencies at 0.5 MHz for the hadronic, electromagnetic (electron, photon, π^0's) and muon triggers. These were obtained after the optimization of the L0 trigger, with the resulting efficiencies being reshown (for easy reference) in the second column. All uncertainties are statistical.

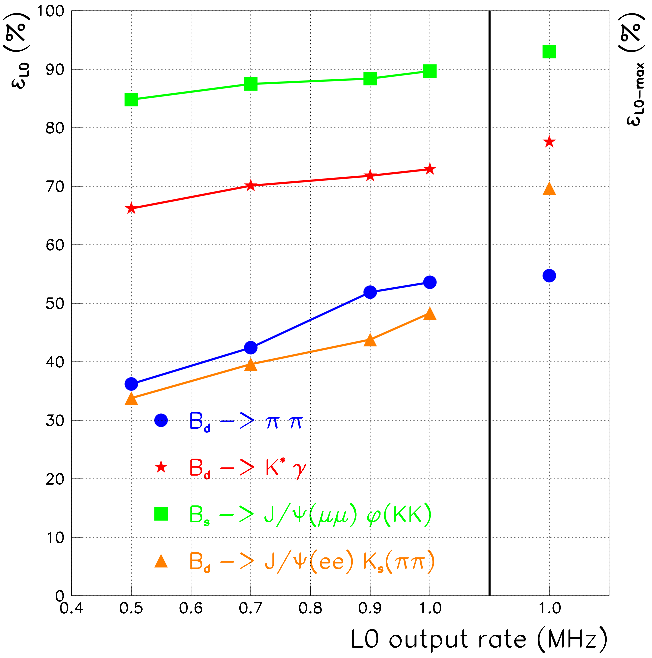

Figure 1: L0 efficiencies (ϵ_{L0}) as a function of the L0 output rate. The last set of data points refers to the maximum efficiency ($\epsilon_{\mathrm{L0-max}}$) obtained after individual optimization of each channel (refer to the text for further details).

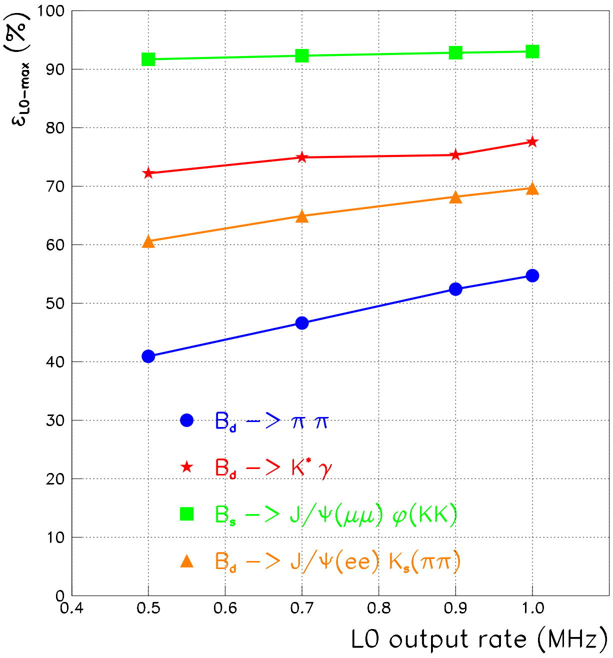

Figure 2: Maximum L0 efficiencies ($\epsilon_{\mathrm{L0-max}}$) as a function of the L0 output rate obtained after individual optimization of each channel (refer to the text for further details).